

8. In seven subjects from four kindreds (FFI 1, IV-37, IV-21, V-58, IV-16; FFI 2, IV-26; FFI 4, III-2; FFI 5, IV-4) sleep was investigated with polysomnography or overnight recording; severe insomnia with marked reduction or loss of slow waves and REM sleep stages was observed (5). In subject FFI 3, IV-7 sleep study revealed an atypical REM sleep pattern (W. Pendlebury, unpublished data). Insomnia was not reported in FFI 3 subjects IV-12 and V-14; the latter, however, was reported to have somnolence, (10). Dysautonomia, was recorded in all but four cases (FFI 3, IV-7, V-14; FFI 4, III-1; and FFI 5, IV-1) (5). Thalamic atrophy affected anterior ventral and mediodorsal nuclei in all 13 cases examined at autopsy. Other thalamic nuclei were variably involved. Cerebral cortex was unremarkable or had a moderate degree of astrogliosis. Widespread spongiosis was present only in two subjects (FFI 1, V-58 and IV-16) who had a clinical course of 25 and 34 months (5). These two subjects also had high-voltage synchronized spike and wave activity in electroencephalogram recording while the others had diffuse slowing (5). A single focus of initial spongiosis was seen in the entorhinal cortex of FFI 5 subject IV-4 who had a course of 13 months (5). Detailed histopathological examination was not carried out in FFI 3 subjects III-5 and IV-12 (10). Transmission of the disease to primates was unsuccessful with brain homogenates from FFI 3 subjects III-5, IV-5, IV-12 (7). Linkage analysis between disease and the Asn¹⁷⁸ mutation carried out in kindred FFI 1 gave a cumulative lod score of 6.16 (5).
9. The Asn¹⁷⁸ CJD subtype is characterized by early and severe memory loss (7). EEG shows diffuse slowing, but no periodic activity (7). Sleep physiological studies were performed in at least one patient with nonspecific findings (P. Brown, unpublished data). Neuropathological examination was carried out at autopsy in subjects CJD-Str III-9, III-14, CJD-Wui IV-4, CJD-Day IV-2, and IV-5, and by biopsy of cerebral cortex in subjects CJD-Str III-6, III-11, and CJD-Bel II-1 (7, 16). There was moderate or severe spongiosis with moderate or mild astrogliosis of the cerebral cortex in all cases. The thalamus was affected by spongiosis in several cases but less severely than the cerebral cortex. Autopsy examination of nine members of the CJD-Wui (IV-2), CJD-Day (III-1; III-7; III-8), CJD-Kui (II-9; II-10; III-4), and CJD-LaP (II-3; II-4) kindreds not included in this study revealed changes similar to those observed in the tested subjects (16, 17). Experimental transmission was accomplished with tissue from subjects CJD-Str III-6; CJD-Wui IV-4; CJD-Day IV-5; CJD-Kui III-8; it was unsuccessful with subject CJD-Bel II-1 (7). Linkage analysis between disease and the Asn¹⁷⁸ mutation carried out in kindreds CJD-Str and CJD-Day gave a cumulative lod score of 5.30 (8).
10. B. W. Little, *Ann. Neurol.* 20, 231 (1986).
11. L. G. Goldfarb *et al.*, *Am. J. Hum. Genet.* 45, A189 (1989); J. Collinge *et al.*, *Lancet* 337, 1441 (1991).
12. M. S. Palmer, A. J. Dryden, J. T. Hughes, J. Collinge, *Nature* 352, 340 (1991).
13. H. F. Baker *et al.*, *Lancet* 337, 1286 (1991).
14. DNA was extracted from blood, frozen brain tissue, or fixed and paraffin-embedded brain tissue by standard techniques. Either a portion or the entire *PRNP* coding region was amplified by the polymerase chain reaction (PCR) under standard conditions (primer sequences available on request). The number of amplification cycles ranged from 25 to 35, depending on the source of the DNA, with each cycle comprised of denaturation at 94°C, annealing at 60°C, and extension at 72°C. Analysis of the genotype was based on digestion of the amplified DNA with TthIII 1 to screen for the Asn¹⁷⁸ mutation and Nsp I or Mae II for analysis of codon 129.
15. Both *PRNP* alleles from an individual were analyzed by restriction enzyme digestion after cloning the amplified DNA (14) into a plasmid vector and identifying the Asn¹⁷⁸ and Asp¹⁷⁸ alleles by digestion with TthIII 1. Complete sequencing of

the *PRNP* coding region was performed for 11 patients. Both alleles were sequenced using Sequenase (version 2.0; U.S. Biochemicals) or Taq DNA polymerase (Applied Biosystems). The resulting sequences were compared to that previously published (18).

16. M. Haltia, J. Kovanen, H. Van Crevel, G. T. Bots, S. Stefanko, *J. Neurol. Sci.* 42, 381 (1979); A. Buge *et al.*, *Rev. Neurol. Sci.* 134, 165 (1978); G. Guidon, thesis, Universite de Rennes (1978); P. Brown, L. Goldfarb, C. Gajdusek, unpublished data.
17. W. W. May, H. H. Itabashi, R. N. DeJong, A. Arbor, *Arch. Neurol.* 19, 137 (1968); P. Brown, L. Gold-

farb, C. Gajdusek, unpublished data.

18. H. A. Kretzschmar *et al.*, *DNA* 5, 315 (1986).
19. We thank F. Cathala, J.-M. Vallat, L. Berg, R. Torack, F. Tagliavini, C. Bugiani, N. Rizzuto, S. Pogacar, and E. Cinti for providing tissue samples; S. Richardson and R. Xue for technical assistance; and S. Bowen for assembling the manuscript. Supported by the National Institute of Neurological and Communicative Disorders and Stroke (NS 14509-13), National Institute on Aging (ADRC AG-08012-02), National Institutes of Health (NIA 1 R01 AGNS08155-02), and the Britton Fund.

14 August 1992; accepted 2 October 1992

Ikaros, an Early Lymphoid-Specific Transcription Factor and a Putative Mediator for T Cell Commitment

Katia Georgopoulos,* David D. Moore, Bruce Derfler

In a screen for transcriptional regulators that control differentiation into the T cell lineage, a complementary DNA was isolated encoding a zinc finger protein (Ikaros) related to the *Drosophila* gap protein Hunchback. The Ikaros protein binds to and activates the enhancer of a gene encoding an early T cell differentiation antigen, CD3 δ . During development, Ikaros messenger RNA was first detected in the mouse fetal liver and the embryonic thymus when hematopoietic and lymphoid progenitors initially colonize these organs; no expression was observed in the spleen or the bone marrow. The pattern of Ikaros gene expression and its ability to stimulate CD3 δ transcription support the model that Ikaros functions in the specification and maturation of the T lymphocyte.

T cell progenitors originate in the bone marrow of the adult and the fetal liver of the embryo and migrate to the thymus where they undergo T cell maturation or apoptosis (1-5). Restriction of a pluripotent progenitor to the lymphoid lineage is the first step toward T cell commitment and occurs outside the thymus. This lymphoid progenitor then commits to the T or the B cell lineage. The mechanisms that control the outcome of these early developmental decisions remain unclear.

Early events in T cell differentiation may be characterized by studying the regulation of transcription of T cell-restricted antigens (6). We examined the transcriptional control of one of the earliest definitive T cell differentiation markers, the CD3 δ gene of the CD3-T cell receptor (TCR) complex (5, 7). In order to identify a transcription factor expressed at, or earlier than, T cell commitment, which could function as a genetic switch regulating entry into the T cell lineage, we characterized the T cell-specific enhancer mediating CD3 δ gene expression (8, 9). This enhancer contains

two functionally distinct elements, δ A and δ B, with T cell-restricted activity (9). Mutational analysis of the δ A element has defined two transcriptionally active binding sites which are required for full activity of the δ A element and the CD3 δ enhancer (Fig. 1, A and B), a CRE [cyclic AMP (adenosine 3',5'-monophosphate) response element]-like region and a G-rich sequence. Three isoforms of the ubiquitously expressed CRE-binding protein (CRE-BP) were cloned from T cells for their ability to interact with the CRE-like binding site of the δ A element (10). Although dominant negative mutations in CRE-BP down-regulate the activity of this enhancer element in T cells, the expression of this transcription factor in all hematopoietic and non-hematopoietic cells suggests that it is unlikely to be the switch that activates the CD3 δ enhancer in the early prothymocyte progenitor (10).

A variant of the δ A element with a mutated CRE binding site (δ Amu1-CRE) was used to screen a T cell expression library as described (10). A lymphoid-restricted cDNA was cloned that encodes a previously uncharacterized zinc finger protein (Ikaros). The Ikaros protein contains 431 amino acids and five CX₂CX₁₂HX₃H zinc finger motifs organized in two separate clusters (Fig. 2A). The first cluster of three fingers is located 59 amino acids from the

K. Georgopoulos and B. Derfler, Cutaneous Biology Research Center, Harvard Medical School, Massachusetts General Hospital, Charlestown, MA 02114. D. D. Moore, Department of Molecular Biology, Harvard Medical School, Massachusetts General Hospital, Boston, MA 02114.

*To whom correspondence should be addressed.

initiating methionine, whereas the second cluster is at the COOH-terminus of the protein, 245 amino acids downstream from the first cluster. Two of the finger modules of this protein deviate from the consensus amino acid composition of the Cys-His family of zinc fingers: Finger 3 in the first cluster and finger 5 at the COOH-terminus have four and five amino acids, respectively, between the histidine residues (Fig. 2A). This arrangement of zinc fingers in two widely separated regions resembles that found in Hunchback, a *Drosophila* segmentation gap protein (11). Searches in the protein database revealed a 43% identity between the second finger cluster of Ikaros

and that of Hunchback. In addition, both second finger clusters are located at the COOH-terminus of these molecules (Fig. 2B). The similarity at the COOH-terminus of these proteins and their finger organization suggests they are members of a conserved subfamily of zinc finger proteins.

The ability of the Ikaros protein to bind to the δA element was examined. The Ikaros protein and a truncated variant that retains the second zinc finger domain bind to the δA element with high affinity (Fig. 1, C and D). Oligonucleotides encoding the wild type δA or δA with mutations outside the G box compete for the binding of the Ikaros proteins (δA , $\delta Amu1$ -CRE;

Fig. 1, A and C), whereas mutations within the G box abrogate Ikaros binding ($\delta Amu2$ -G box; Fig. 1, C and D).

In the adult mouse, Ikaros mRNA is restricted to the thymus and the spleen, with threefold higher expression in the thymus than in the spleen (Fig. 3, A and B). Spleen preparations depleted of T cells (TDSC) expressed little of this message when compared to normal thymocytes (Fig. 3B). The restricted and differential expression of the Ikaros gene in the thymus and spleen and the high degree of enrichment in thymocytes relative to that of splenic lymphocytes suggest Ikaros may function to regulate gene expression in T cells and their

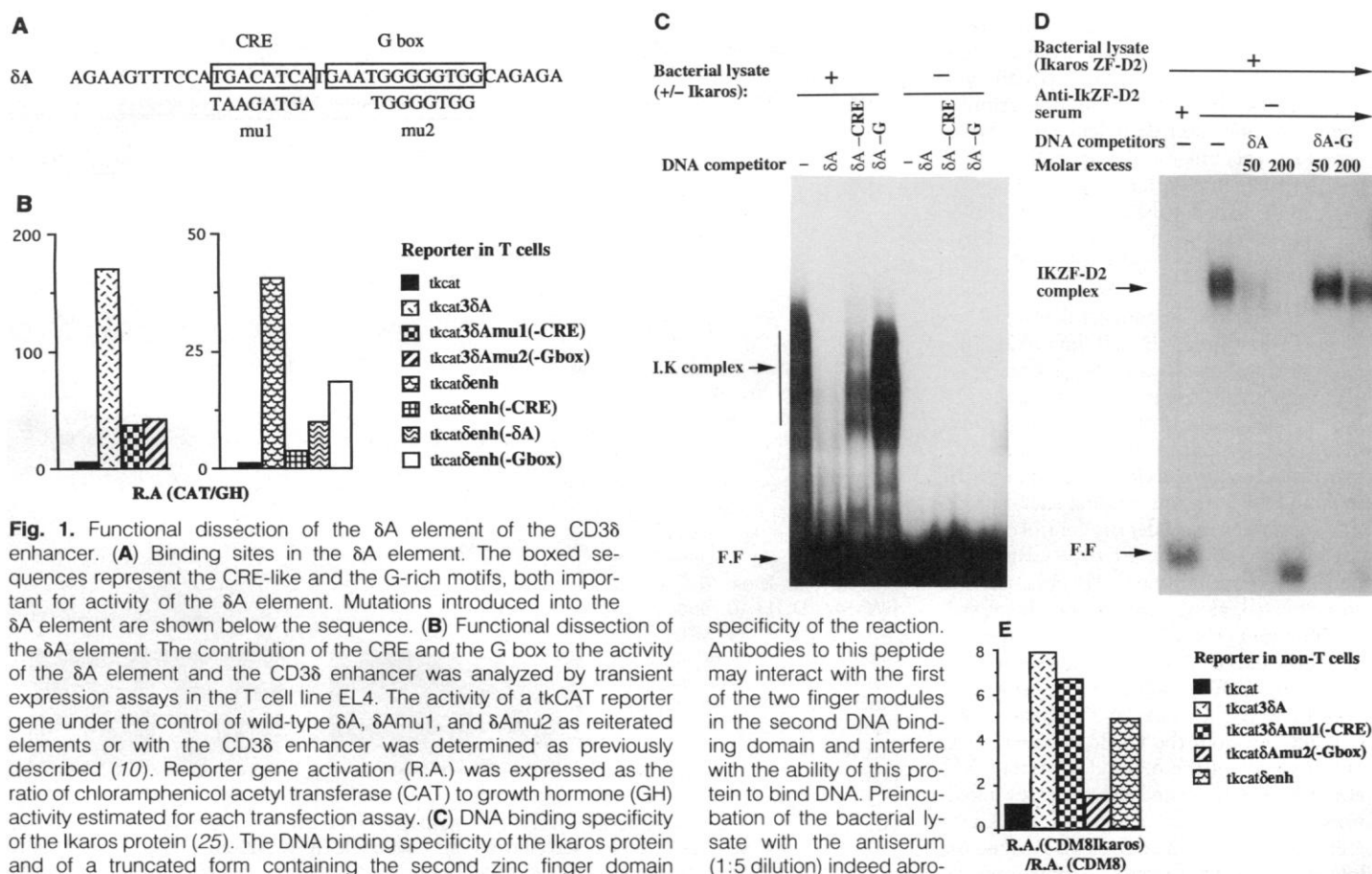


Fig. 1. Functional dissection of the δA element of the CD3 δ enhancer. **(A)** Binding sites in the δA element. The boxed sequences represent the CRE-like and the G-rich motifs, both important for activity of the δA element. Mutations introduced into the δA element are shown below the sequence. **(B)** Functional dissection of the δA element. The contribution of the CRE and the G box to the activity of the δA element and the CD3 δ enhancer was analyzed by transient expression assays in the T cell line EL4. The activity of a tkCAT reporter gene under the control of wild-type δA , $\delta Amu1$, and $\delta Amu2$ as reiterated elements or with the CD3 δ enhancer was determined as previously described (10). Reporter gene activation (R.A.) was expressed as the ratio of chloramphenicol acetyl transferase (CAT) to growth hormone (GH) activity estimated for each transfection assay. **(C)** DNA binding specificity of the Ikaros protein (25). The DNA binding specificity of the Ikaros protein and of a truncated form containing the second zinc finger domain (IKZF-D2 amino acids 197 to 431) were tested in a gel retardation assay. Bacterial lysates (4 μ g) expressing the Ikaros protein were incubated with a radiolabeled oligonucleotide (100,000 cpm) encoding the δA element. A 50-fold excess of wild-type δA competed effectively for Ikaros binding. The $\delta Amu1$ oligonucleotide with a wild-type G box and a mutant CRE binding site competed effectively but to a smaller degree than wild type, indicating that flanking sequences to the G box are also important in determining binding specificity. In contrast, the $\delta Amu2$ with a 1-bp deletion in the G box did not compete for binding of the Ikaros protein to the wild-type oligonucleotide. Bacterial lysates not expressing the Ikaros protein were used as a control. **(D)** DNA binding specificity of a truncated Ikaros protein. A truncated Ikaros protein (IKZF-D2, amino acids 197–431) containing the second but not the first finger domain was also tested for binding specificity. Bacterial lysates (0.4 μ g) expressing the truncated protein (amino acids 197–431) were incubated with 10,000 cpm of radiolabeled δA oligonucleotide. An antiserum raised to an Ikaros peptide (amino acids 300–399) from this region was used to determine the

specificity of the reaction. Antibodies to this peptide may interact with the first of the two finger modules in the second DNA binding domain and interfere with the ability of this protein to bind DNA. Preincubation of the bacterial lysate with the antiserum (1:5 dilution) indeed abrogated binding of the truncated Ikaros protein to the δA site. No such effect was detected when bacterial lysates expressing other DNA binding proteins were tested (18). A 50- and 200-fold molar excess of the δA and δA -G binding sites were used as competitors. A 50-fold molar excess of the δA site was sufficient to compete most of the Ikaros binding; in contrast, the δA -G site was not able to compete at a 200-fold excess. The full-length Ikaros-DNA binding complex appears to migrate in the gel assays as a smear whereas the truncated protein complex migrates as a single band. This may be due to the presence of two DNA binding domains in this molecule and moreover may indicate complex protein-protein-DNA interactions. **(E)** Expression of the Ikaros gene in non-T cells up-regulates the activity of the δA element. The CDM8 and CDM8 Ikaros recombinant expression vectors were cotransfected with the *tkcat*, *tkcat3delta*, *tkcat3deltaAmu1*, *tkcat3deltaAmu2*, and *tkcatdeltaenh* reporter genes into CV1 (kidney epithelial) cells as described previously (10). The ratio of reporter activation (R.A. = CAT/GH) in the presence and absence of Ikaros expression was estimated.

progenitors. Examination of Ikaros expression in cell lines supports this hypothesis. The Ikaros mRNA was detected in a number of T lymphoma cell lines. The mature T cell line EL4 contained the highest amounts of Ikaros mRNA, whereas DO11.10, BW5147, and SL12.1 lymphomas showed moderate to low expression. Little or no mRNA was detected in cell lines representing other hematopoietic lineages, including the bone marrow-derived progenitor cell line FDCP1 which exhibits myeloid morphology and differentiation potential, the mast cell line RBL, the macrophage line J774 (Ikaros mRNA expression is 1/25 of that in thymocytes), and mouse proerythro leukemia (MEL) cells induced to differentiate into the erythroid lineage (Fig. 3B). Nevertheless, moderate amounts of Ikaros mRNA were detected in undifferentiated MEL cells and in the B cell lymphoma A20 (Fig. 3B). Immortalization of these cell lines and their leukemic phenotype may account for the apparently aberrant expression of this nuclear factor in these cells. Ikaros mRNA is not expressed in large amounts in normal B cells (T cell-depleted spleen cells, Fig. 3B) or in erythroid progenitors in vivo (in situ data, Fig. 4). Moderate amounts of Ikaros mRNA in the transformed B cell line A20 may reflect expression in an early lymphoid progenitor that has the potential to differentiate into either the T or the B cell lineage.

We next examined whether Ikaros protein that bound to the δA element could activate transcription from this binding site. The tk-CAT reporter gene under the control of either a reiterated δA binding site (+/-CRE/-G) or under the control of the CD3 δ enhancer was cotransfected, along with a recombinant vector containing the Ikaros gene, into the kidney epithelial cell line CV1. Expression of the Ikaros gene in CV1 cells stimulated transcription from the G box of a reiterated δA element and from the CD3 δ enhancer (Fig. 1E). Activity of the δA and $\delta Amu1(-CRE)$ elements was stimulated eight- and sevenfold, respectively, whereas activity of the CD3 δ enhancer was stimulated fivefold. Because the CD3 δ enhancer contains at least two regulatory elements, expression of the transcription factors that bind to these sites is necessary for its full activation potential. Ikaros gene expression did not significantly stimulate the activity of the thymidine-kinase promoter or of the $\delta Amu2(-G)$ element (Fig. 1E). Thus, the Ikaros gene can control activity of the T cell-specific δA element of the CD3 δ enhancer and can mediate expression of the CD3 δ gene in T cells.

In the adult mouse, the Ikaros gene is strongly expressed in T cells and their progenitors. To determine whether the Ikaros gene is expressed before lymphoid differentiation in the thymus, and whether

Fig. 2. Amino acid sequence of the protein encoded by the Ikaros cDNA and homology to the *Drosophila* gap protein Hunchback. (A) The boxed amino acid sequence indicates the Ikaros zinc finger domains. (B) Similarity between the COOH-terminal zinc finger domains of the Ikaros and Hunchback proteins. Protein alignment was performed with the Gap program of the University of Wisconsin sequence analysis software. *-stop codon. Abbreviations for the amino acid residues are: A, Ala; C, Cys; D, Asp; E, Glu; F, Phe; G, Gly; H, His; I, Ile; K, Lys; L, Leu; M, Met; N, Asn; P, Pro; Q, Gln; R, Arg; S, Ser; T, Thr; V, Val; W, Trp; and Y, Tyr.

A

```

1  MetAspValAspGluGlnAspMetSerGlnValSerGlyLysGluSerProProVal
21  SerAspThrProAspGluGlyAspGluProMetProValProGluAspLeuSerThrThr
41  SerGlyAlaGlnGlnAsnSerLysSerAspArgGlyMetGlyGluArgProPheGlyCys
61  AsnGlnCysGlyAlaSerPheThrGlnLysGlyAsnLeuLeuArgHisIleLysLeuHis
81  SerGlyGluLysProPheLysCysHisLeuCysAsnTyrAlaCysArgArgArgAspAla
101  LeuThrGlyHisLeuArgThrHisSerValGlyLysProHisLysCysGlyTyrCysGly
121  ArgSerTyrLysGlnArgSerSerLeuGluGluHisLysGluArgCysHisAsnTyrLeu
141  GluSerMetGlyLeuProGlyValCysProValIleLysGluGluThrAsnHisAsnGlu
161  MetAlaGluAspLeuCysLysIleGlyAlaGluArgSerLeuValLeuAspArgLeuAla
181  SerAsnValAlaLysArgLysSerSerMetProGlnLysPheLeuGlyAspLysCysLeu
201  SerAspMetProTyrAspSerAlaAsnTyrGluLysGluAspMetMetThrSerHisVal
221  MetAspGlnAlaIleAsnAsnAlaIleAsnTyrLeuGlyAlaGluSerLeuArgProLeu
241  ValGlnThrProProGlySerSerGluValValProValIleSerSerMetTyrGlnLeu
261  HisLysProProSerAspGlyProProArgSerAsnHisSerAlaGlnAspAlaValAsp
281  AsnLeuLeuLeuSerLysAlaLysSerValSerSerGluArgGluAlaSerProSer
301  AsnSerCysGlnAspSerThrAspThrHisSerAsnAlaGluGluGlnArgSerGlyLeu
321  IleTyrLeuThrAsnHisIleAsnProHisAlaArgAsnGlyLeuAlaLeuLysGluGlu
341  GlnArgAlaTyrGluValLeuArgAlaAlaSerGluAsnSerGlnAspAlaPheArgVal
361  ValSerThrSerGlyGluGlnLeuLysValTyrLysCysGluHisCysArgValLeuPhe
381  LeuAspHisValMetTyrThrIleHisMetGlyCysHisGlyCysHisGlyPheArgAsp
401  ProPheGluCysAsnMetCysGlyTyrHisSerGlnAspArgTyrGluPheSerSerHis
421  IleThrArgGlyGluHisArgTyrHisLeuSer

```

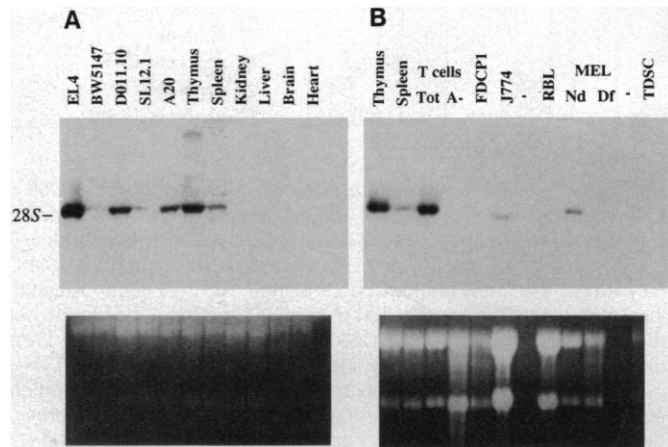
B

```

Ikaros 370 VYKCEHCRVLEFLDHVMTIHMGGCHGFRDPFCNMGYHSQDRYEFSSHITRGEHYHLS*431
Hunchback 704 LYECKYCDIFPKDVLVYTIHMGGVHSCD...DVFKNMGCEKCDGPGVGLFVHMARNH...S*758

```

Fig. 3. Tissue-specific expression of the Ikaros gene. The tissue distribution of the Ikaros gene was determined by Northern (RNA) hybridization of total RNAs (15 μ g per sample) prepared from (A) T lymphoma cell lines EL4, BW5147, DO11.10, and SL12.1; the B cell lymphoma A20; and adult thymus, spleen, kidney, liver, brain, and heart and from (B) thymus, spleen, thymocytes (total and polyadenylated RNA), bone marrow-derived stem



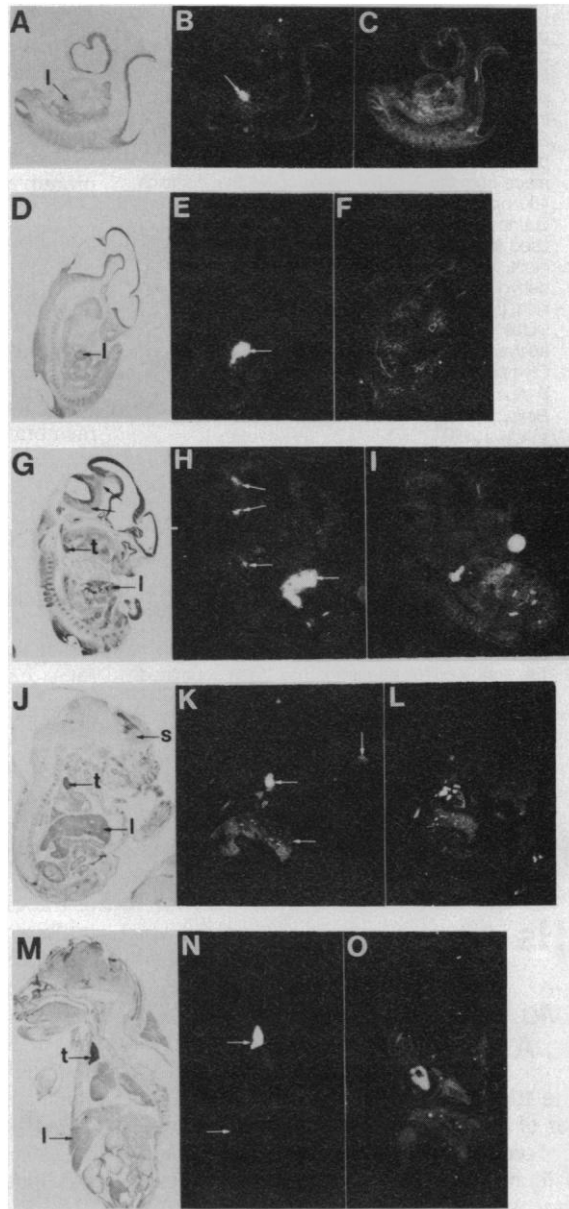
cell progenitors FDCP1, macrophage cell line J774, mast cell line RBL, undifferentiated MEL, 58-hour DMSO-induced MEL cells, and T-depleted spleen cells (TDSC). A 300-bp fragment from the 3' untranslated region of the Ikaros cDNA was used as a probe. The lower panels of (A) and (B) show the 28S and 18S RNAs detected on the Northern membranes under ultraviolet light after the probe.

it may be responsible for mediating gene expression in T cell progenitors, we used in situ hybridization to study its expression during hematopoiesis in the mouse embryo.

The first hematopoietic center in the mouse embryo is the yolk sac, formed about day 7 of gestation and heavily populated at this time with primitive erythroblasts (12-16). In contrast to the erythroid-specific transcription factor GATA-1 (17) the Ikaros mRNA was not detected in the yolk sac at day 8 (18). In the embryo proper,

expression of Ikaros RNA was first detected in the liver rudiment at the onset of its development as a hematopoietic center [day 9.5 to 10.5, Fig. 4, A to F (12-16)]. At this time, pluripotent stem cells and more restricted progenitors are found in this tissue that can successfully reconstitute irradiated animals with the complete spectrum of hematopoietic lineages (19-24). The large amount of Ikaros mRNA detected in the early fetal liver began to decline after day 14 (Fig. 4, G to O), although this tissue

Fig. 4. In situ hybridization in the developing mouse embryo (26, 27). Bright-field view of sections hybridized with an Ikaros antisense-RNA probe (**A, D, G, J, M**), dark-field view of sections hybridized with Ikaros antisense-RNA probe (**B, E, H, K, N**), dark-field of sections hybridized with Ikaros sense-RNA probe (**C, F, I, L, O**). (**A, B, C**) Day 9.5. Ikaros RNA is first detected in the liver primordium. (**D, E, F**) Day 10.5. Ikaros RNA amounts are higher in the developing liver rudiment. (**G, H, I**) Day 12. Ikaros RNA is detected in the thymic rudiment and in distinct cells of the brain. (**J, K, L**) Day 16. Ikaros RNA amounts are higher in the thymus and the proximal corpus striatum, whereas RNA levels in the liver are lower. (**M, N, O**) Day 19. The thymus appears to be the major site of expression of Ikaros RNA and in the liver Ikaros RNA is not detected above background. In more lateral sections, expression in the corpus striatum is still detectable. Arrows indicate the hybridizing tissues. l, Liver; t, thymus; s, striatum. Certain areas in the embryo such as the heart tissue reflect light under dark field illumination at low magnification. This is seen in both the antisense and sense panels and does not represent a real hybridization signal. Examination of these tissues under high magnification reveals no hybridization signal over these cells.



remains the major site for erythropoiesis, myelopoiesis, and B cell development through mid-gestation and is active past birth. The lower expression of Ikaros in the fetal liver at mid-gestation correlates with a shift in the population of hematopoietic progenitors in this organ from pluripotent stem cells to more committed erythroid progenitors. The decrease of Ikaros mRNA in the fetal liver is concomitant with a dramatic increase in expression in the developing thymus.

Beginning at day 12, when lymphopoietic stem cells are first colonizing this organ, Ikaros mRNA was readily detected in the thymic rudiment (Fig. 4, G to I) (1-3, 24). A group of cells expressing high amounts of Ikaros mRNA was detected at the center of the thymic rudiment and was surrounded by non-expressing cells in the

periphery (18). Expression in the developing thymus became prominent by day 16, and by day 19, this organ was the major site of expression of the Ikaros gene (Fig. 4, J to O). The Ikaros mRNA was detected in lymphoid cells throughout the thymus, with quantities in the medulla being slightly more elevated than those in the cortex (18).

Ikaros RNA expression was first detected in embryonic spleen during late gestation at low concentrations when compared to the thymus (day 19) (18). Although the spleen is active in erythropoiesis, myelopoiesis, and B cell differentiation from mid-gestation, its population with mature T cells from the thymus begins late in embryogenesis and may correlate with the late expression of the Ikaros gene in this organ (16). No expression of the Ikaros message was

detected in the bone marrow of the long bones or the spinal column at day 19. In contrast, RNA for the myeloid-specific factor *Spy1* (28) and the erythroid factor *GATA-1* (17), was both abundantly expressed in the bone marrow and spleen at this time. The only other site in the mouse embryo that exhibited Ikaros expression was a restricted group of cells in the brain (day 12) that gives rise to the proximal corpus striatum (days 16 to 19).

In situ studies on the Ikaros gene in the developing mouse embryo were consistent with the expression pattern observed in primary cells and cell lines in the adult mouse. Ikaros mRNA was highly enriched in embryonic and adult thymus. In the mouse embryo the low amounts of expression detected in hematopoietic centers active in erythropoiesis, myelopoiesis, and B cell development from mid- to late gestation were consistent with the pattern of expression observed in hematopoietic cells and cell lines in the adult. Prominent amounts of Ikaros mRNA were detected in the early liver primordium at a time when it is being populated with primitive hematopoietic stem cells. Large quantities of Ikaros mRNA may be necessary in the pluripotent hematopoietic stem cell for further commitment and differentiation into the lymphoid and ultimately the T cell progenitor. A decrease in Ikaros expression in this hematopoietic center from mid- to late gestation may reflect changes in the developmental profile of hematopoietic progenitors in this organ. The comparatively low amounts of Ikaros mRNA expression in sites of adult and embryonic B cell development suggest a primary role in the regulation of gene expression in the T lymphocyte. The ability of the lymphoid-restricted transcription factor Ikaros to stimulate the transcription of an early T cell differentiation marker and its enriched expression in sites of adult and embryonic thymopoiesis support the model that Ikaros functions in the specification and maturation of the T lymphocyte.

REFERENCES AND NOTES

1. M. A. S. Moore and J. J. T. Owen, *J. Exp. Med.* **126**, 715 (1967).
2. R. Auerbach, J. S. Cairns, N. Roehm, *Fortschr. Zool.* **26**, 287 (1981).
3. J. J. T. Owen and E. J. Jenkinson, *Prog. Allergy* **29**, 1 (1981).
4. H. Von Boehmer, *Annu. Rev. Immunol.* **6**, 309 (1988).
5. B. F. Haynes, S. M. Denning, K. H. Singer, J. Kutzenberg, *Immunol. Today* **10**, 87 (1989).
6. J. M. Leiden, *ibid.* **13**, 22 (1992).
7. A. J. Furlley *et al.*, *Cell* **46**, 75 (1986).
8. K. Georgopoulos, P. van den Elsen, E. Bier, A. Maxam, C. Terhorst, *EMBO J.* **7**, 2401 (1988).
9. K. Georgopoulos, D. Galson, C. Terhorst, *ibid.* **9**, 109 (1990).
10. K. Georgopoulos, B. Morgan, D. D. Moore, *Mol. Cell. Biol.* **12**, 747 (1992).
11. D. Tautz *et al.*, *Nature* **327**, 383 (1987).
12. E. S. Russel, *Adv. Genet.* **20**, 357 (1979).

13. J. E. Barker, *Dev. Biol.* **15**, 14 (1968).
14. P. M. C. Wong and C. J. Eaves, *Proc. Natl. Acad. Sci. U.S.A.* **83**, 3851 (1986).
15. D. Metcalf, *Molecular Control of Blood Cells* (Harvard Univ. Press, Cambridge, 1987).
16. R. Rugh, *The Mouse: Its Reproduction and Development* (Oxford Univ. Press, New York, 1991), pp. 272–275.
17. E. Whitelaw, S-F. Tsai, P. Hogben, S. H. Orkin, *Mol. Cell. Biol.* **10**, 6596 (1990).
18. K. Georgopoulos, unpublished material.
19. K. Ikuta *et al.*, *Cell* **62**, 863 (1990).
20. C. T. Jordan, J. P. McKearn, I. R. Lemischka, *ibid.* **61**, 953 (1990).
21. S. J. Szilvassy *et al.*, *Proc. Natl. Acad. Sci. U.S.A.* **86**, 8798 (1989).
22. B. Capel, R. Hawley, L. Covarrubias, T. Hawley, B. Mintz, *ibid.*, p. 4564.
23. C-P. Liu and R. Auerbach, *Development* **113**, 1315 (1991).
24. _____, *Eur. J. Immunol.* **21**, 1849 (1991).
25. The full length and truncated Ikaros proteins were expressed in the *E. coli* BL21 strain from the pet3a vector. One microliter of a 1:4 and of a 1:40 dilution of bacterial lysate (approximately 4 and 0.4 μ g of total protein) that expressed Ikaros and Ikaros ZF-D2 were used respectively in a gel retardation assay with 100,000 and 10,000 cpm of kinased double-stranded oligonucleotide encoding the δ A element as described previously (10). A 1:4 dilution of bacterial lysate programmed with wild-type pet3a vector was used as a control. A 50- and 200-fold molar excess of unlabeled double stranded oligonucleotides encoding δ A wild-type and mutant variants were used as competitors.
26. Embryos were harvested from timed, pregnant CD1 mice (Charles River) and were fixed in 4% paraformaldehyde for 2 hours to 2 days depending on size. A series of dehydration steps was performed in alcohols followed by xylenes before paraffin embedding (27). Sections were prepared and treated according to published protocols (27). Sense and antisense 32 P-UTP (uridine 5'-diphosphate)-labeled RNA probes 320 bp in size were made from the 3' of the Ikaros cDNA that contains 100 bp of coding and 220 bp of untranslated sequence (1230 to 1550 bp of Ikaros cDNA) and were used to hybridize to selected slides at 48°C overnight. After high-stringency washing, slides, were dehydrated, dipped in diluted photographic emulsion (NBT2), and exposed for 3 weeks. Dipped slides were developed, stained with Giemsa, and analysed by bright- and dark-field illumination on an Olympus dissecting microscope.
27. F. Ausubel *et al.*, *Current Protocols in Molecular Biology* (Wiley-Interscience, New York, 1991), pp. s14.1–s14.6.
28. D. Galson, manuscript in preparation.
29. We thank D. Dietch and R. Bruns for advice and help with in situ studies; D. Galson, J. Hensold, and M. Gurish for MEL, RBL, and J774 RNA, respectively; S. Grabee for preparing T-depleted splenic B cells; and B. Morgan and P. Goetinck for critical discussions and comments. This work was supported by a Shisheido grant to the Cutaneous Biology Research Center and from the Leukemia Society of America (to K.G.).
30. The Ikaros cDNA sequence has been submitted to GenBank. The accession number is L03547.

2 June 1992; accepted 10 September 1992

A GDP Dissociation Inhibitor That Serves as a GTPase Inhibitor for the Ras-Like Protein CDC42Hs

Matthew J. Hart, Yoshiro Maru, David Leonard, Owen N. Witte, Tony Evans, Richard A. Cerione*

Members of the family of Ras-related guanosine triphosphate (GTP) binding proteins appear to take part in the regulation of a number of biological processes, including cell growth and differentiation. Three different classes of proteins that regulate the GTP binding and GTP hydrolytic activities of the Ras family members have been identified. These different regulatory proteins inhibit guanosine diphosphate (GDP) dissociation (designated as GDIs), stimulate GDP dissociation and GDP-GTP exchange (designated as GDSs), or stimulate GTP hydrolysis (designated as GAPs). In the case of the Ras-like protein CDC42Hs, which is the human homolog of a *Saccharomyces cerevisiae* cell division cycle protein, the GDI protein also inhibited both the intrinsic and GAP-stimulated hydrolysis of GTP. These findings establish an additional role for the GDI protein—namely, as a guanosine triphosphatase (GTPase) inhibitory protein for a Ras-like GTP binding protein.

The GTP binding and GTP hydrolytic (GTPase) activities of the Ras-like GTP binding proteins are essential for their nor-

M. J. Hart, D. Leonard, R. A. Cerione, Department of Biochemistry, Cell, and Molecular Biology and Department of Pharmacology, Schurman Hall, Cornell University, Ithaca, NY 14853.

Y. Maru and O. N. Witte, Department of Microbiology and Molecular Genetics and Molecular Biology Institute, Howard Hughes Medical Institute, University of California, Los Angeles, CA 90024.

T. Evans, Department of Cell Biology, Genentech Inc., 460 Point San Bruno Boulevard, South San Francisco, CA 94080.

*To whom correspondence should be addressed.

mal regulation and function. The exchange of bound GDP for GTP is influenced by GDS proteins, which stimulate GDP dissociation, and by GDI proteins, which inhibit GDP dissociation. GDIs also influence the cellular localization of the Ras-like proteins by stimulating the release of GTP binding proteins from membranes (1–3). Both GDS and GDI activities have been identified for the Ras-like protein CDC42Hs (3, 4). The *dbl* oncogene product (5, 6) serves as a CDC42Hs-GDS (4), whereas a 28-kD protein, purified from bovine brain, serves as

the GDI protein (3). The latter protein appears to be structurally very similar, if not identical, to a protein that attenuates the dissociation of GDP from the Rho (2, 7) and Rac (8) GTP binding proteins.

The regulatory effects of GDI on the Rho protein may result from a specific interaction between the GDI protein and the GDP-bound form of Rho (2). However, the GDI protein elicits a weak but measurable (~10%) inhibition of the dissociation of guanosine-5'-O-(3-thiotriphosphate) (GTP- γ -S) from CDC42Hs (3) and causes the release of the GTP- γ -S-bound CDC42Hs (as well as the GDP-bound CDC42Hs) from membranes (3). This raised the question of whether the GDI protein might alter functional properties of the GTP-bound CDC42Hs species. The results presented below demonstrate an additional regulatory activity for the GDI protein—specifically, the inhibition of the GTP hydrolytic activity of CDC42Hs.

Figure 1A shows that in the presence of GDI (~1 μ g), the rate of the intrinsic GTPase activity of the platelet CDC42Hs (~0.2 μ g) was significantly inhibited. After 12 min at room temperature, less than 40% of the bound [γ - 32 P]GTP was hydrolyzed by CDC42Hs in the presence of the GDI protein, whereas greater than 70% of the GTP was hydrolyzed by CDC42Hs in the absence of the GDI protein. The GDI protein also inhibited the rate of the GTPase activity of CDC42Hs that had been stimulated by the human platelet CDC42Hs-GTPase activating protein (GAP) (9). When an identical set of experiments was performed with [α - 32 P]GTP, there was no difference in the amount of labeled GTP that remained associated with the platelet CDC42Hs in the presence or absence of the GDI protein or the platelet CDC42Hs-GAP (Table 1). These results indicated that the effects of the GDI and CDC42Hs-GAP proteins on the association of labeled GTP were in fact specific for the hydrolysis of GTP [and the release of inorganic phosphate (32 P_i)] and did not reflect changes in the rate of dissociation of GTP. We find a similar inhibition of the GTPase activity of CDC42Hs by the GDI protein (10) when the CDC42Hs was denatured with 10% trichloroacetic acid before quantitation of the release of 32 P_i by extraction with ammonium molybdate and isobutanol plus benzene (11). This indicates that the GDI protein inhibits the GTP hydrolytic event and not the release of 32 P_i from CDC42Hs.

The inhibition of the GTPase activity by the GDI protein was assayed in parallel with the inhibition of [3 H]GDP dissociation throughout the purification of the GDI protein from bovine brain cytosol. At all stages of the purification, the inhibition of the intrinsic GTPase activity of CDC42Hs